て，miR-122がその発現量全体の70%を占めるほど多量に存在しており，miR-122が肝細胞の特徴を制御していると言っても過言ではない[4]。これはmiR-122の発現が肝細胞特異的転写因子であるhepatocyte nuclear factor-4α(HNF-4α)で制御されていることからも窺われる。miR-122は肝細胞の脂質代謝に寄与することが明らかにされているが，最近，miR-122がhepatitis C virus(HCV)の複製に寄与することから，miR-122を用いた治療が考案されている。すなわち，miR-122はHCVゲノムの5'非翻訳領域に存在するS1，S2と呼ばれる標的部位に結合する。miR-122-HCV結合体が形成されるとHCVゲノムは酵素的に分解されることがなくなり増殖が容易になることや宿主の自然免疫機構による排除から逃れることができるようになり安定化される[5]。薬剤として開発されたmiravirsenはmiR-122に対するアンチセンスオリゴヌクレオチドであり，miR-122と特異的に結合してその機能を抑制する。ヒトに対する第2相臨床試験でmiravirsenが血液中HCV-RNAを低下させることが明らかにされ，今後の動向が注目される[6]。

肝がんの病態にmiRNAが関与することも多数の報告により明らかにされてきた。肝臓においてmiR-151はがん誘発性のあるmicroRNAであるoncomirとされた。miR-199a/b-3pは肝がんで発現が低下しており，PAK4-Raf-MEK-ERK経路を阻害することで肝がん細胞の増殖を阻害すると報告された。数種の報告を総合すると肝がんではlet-7，miR-122，miR-26とmiR-101が発現低下しており，一方，miR-221，miR-181とmiR-17-92が発現上昇する[7]。miR-21は乳房，大腸，肺，膵臓，前立腺，胃などヒトの他臓器のがんでもoncomirとして機能することが知られている。miR-21の増加はPTENを活性化し，phosphatidylinositol 3-kinaseからAktへ至るシグナルの活性化に寄与し，肝がんを増殖させる[8]。

胆管細胞がんは肝がんに次いで2番目に多い原発性肝がんである。miR-21やその他多数のmiRNAが胆管細胞がんでも発現上昇しており，programmed cell death 4やtissue inhibitor of metalloproteinase 3を制御している。また，それらのmiRNAはゲムシタビンで誘導されるアポトーシスをPTEN-依存性のphosphatidylinositol 3-kinase活性化により抑制させることが知られている[9]。

Ⅲ　肝線維化における星細胞の役割とmicroRNA

肝炎ウイルスの感染やアルコール，脂肪沈着などで肝細胞が壊死して脱落すると，局所に微小な出血が生じ，血小板凝集とフィブリン形成で一時的に傷が塞がれる。傷害肝細胞，類洞内皮細胞や血小板からはケモカイン，transforming growth factor-β(TGF-β)，platelet-derived growth factor(PDGF)などのメディエーターが産生される。これらに呼応して，末梢血中の好酸球，好中球，リンパ球，マクロファージなどがインターロイキン1(interleukin 1，IL-1)，IL-6，IL-8，IL-10，IL-18，tumor necrosis factor α(TNF-α)やマトリックスメタロプロテアーゼ(matrix metalloproteinase；MMP)などの生理活性物質を産生しつつ炎症局所に集積する。さらに肝類洞に存在する星細胞，類洞内皮細胞やKupffer細胞が活性化して一過性の局所炎症を増幅させる[10]。

星細胞は生理的状況では三次元的に類洞を包囲し，ビタミンAを貯蔵する肝組織特異的pericyte(周皮細胞)と言えるが，炎症時にはα-平滑筋アクチンに代表される分子マーカーを発現するようになり筋線維芽細胞(myofibroblast；MFB)様の細胞へと形質を変え，TGF-βの産生と活性化を介したⅠ型，Ⅳ型コラーゲン産生，vascular endothelial cell growth factor(VEGF)の産生，tissue inhibitor of matrix metalloproteinase(TIMP)の分泌を行う。これにより炎症局所に基底膜様構造を構築し，肝細胞再生の土台を作り，血管新生を伴いながら組織修復を行う。これが急性肝炎のように炎症が一過性で終焉した場合のシナリオである(図1)。

しかしながら，肝炎ウイルス感染や脂肪性肝炎のように炎症が慢性化してしまうと，activator protein 1(AP-1)やc-Jun N-terminal kinase(JNK)などの転写因子の持続活性化と共に星細胞も持続活性化し，MFB様の細胞としてTGF-βの

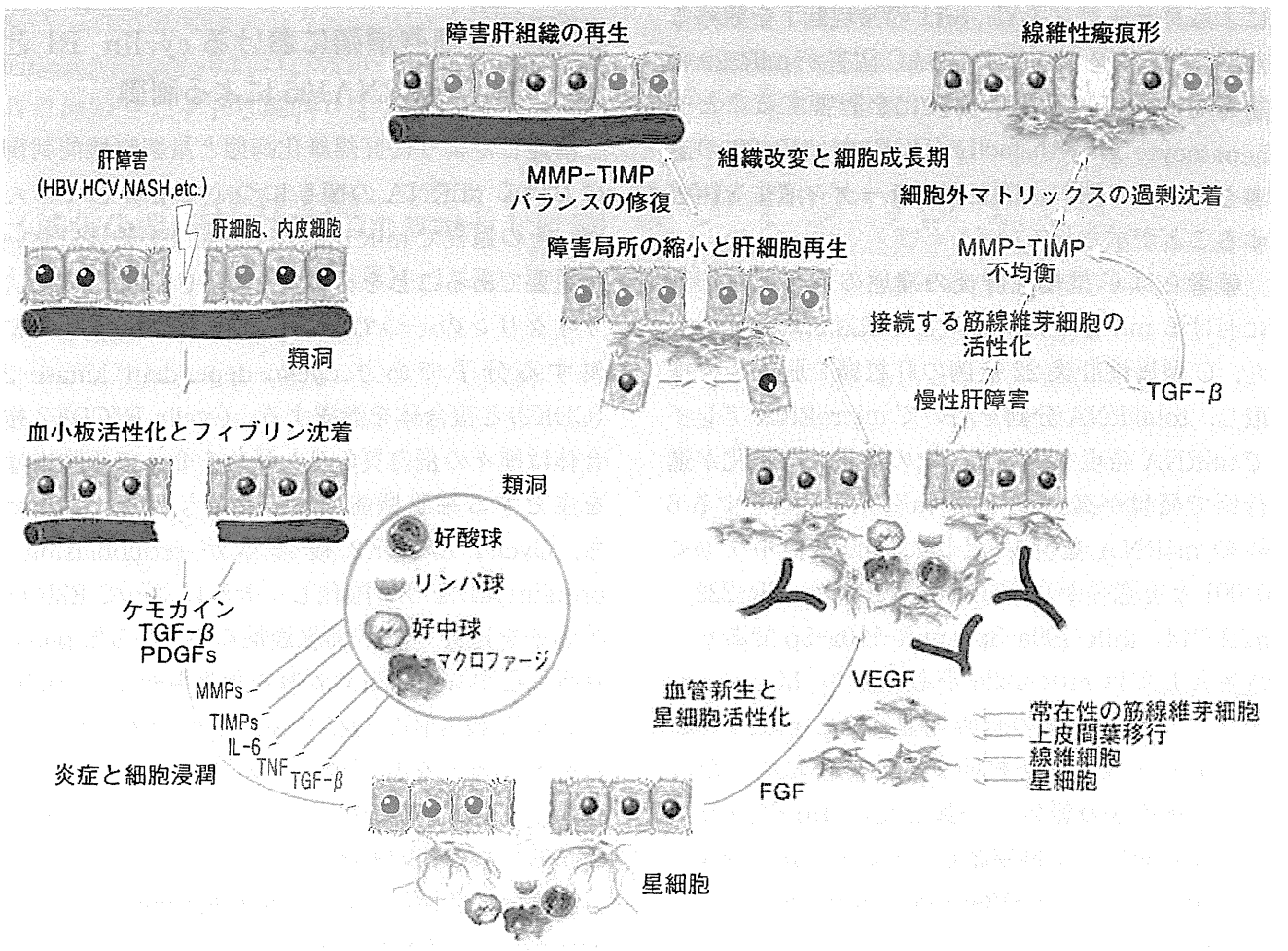

図1　肝障害と治癒過程ならび線維化が生じるメカニズムを示す模式図

産生・活性化とそれを介するTIMP-1過剰産生が生じ，TIMP-1とMMPsとの相対的アンバランスが生じて組織にⅠ型コラーゲンが蓄積することになる。また，MFBはnuclear factor κB(NFκB)やphosphoinositide 3-kinase-Akt経路の活性化により細胞死抵抗性となり，新生血管の構築を伴いながら線維性隔壁を構成して瘢痕形成を行う。また，MFB化した星細胞はmacrophage chemotactic protein(MCP)，macrophage inflammatory protein(MIP)，CCやCXCなどのケモカイン産生，抗原提示，toll-like receptor 4(TLR4)やCD14の発現を伴ったエンドトキシンへの高反応性を介して，O_2^-，nitric oxideなどの活性酸素種を産生させ，局所炎症を持続させる。さらに，星細胞以外の門脈域MFB，中皮由来のMFB，線維細胞，骨髄由来の細胞群らが線維性隔壁構成に加わる。これらが同時進行して組織硬度が増し，組織が改築してゆく[11]。

星細胞機能に及ぼすmiRNAについては近年急速に報告が増加している。miR-29は多種類のコラーゲンmRNAの3' UTR領域に結合するmiRNAであり，コラーゲン遺伝子発現を調節する。ラットから分離した初代培養星細胞を用いた検討からmiR-29bは星細胞の活性化と伴に発現低下することが観察された。miR-29bを星細胞に強制発現させるとⅠ型コラーゲンの発現抑制と伴に星細胞の活性化自体が抑制された[12]。Kweiecinskiらは星細胞におけるplatelet-derived growth factor-CやinsulinlikegrowthfactorⅠの発現がmiR-29で減少すると報告した[13]。Roderburgらはヒト肝組織を用いてmiRNAを測定し，miR-29ファミリーが線維化の進行と伴に発現低下することを報告した。同様にBandyopadhyayらはHCV感染によるヒトの肝組織miR-29の発現低下，HCV感染による肝細胞のmiR-29発現低下，LX-2細胞におけるmiR-29過剰発現

によるコラーゲン1A1，3A1の発現低下を観察した[14]。一方，クラスⅡのHDAC阻害がmiR-29の誘導を介して星細胞の活性化を阻害することやhepatocyte growth factor(HGF)がmiR-29の誘導を介してⅠ型およびⅣ型コラーゲン産生を阻害することが示されている。

筆者らはC型慢性肝炎の病態の進行度と肝臓におけるmiRNA発現に関して検討した。すなわち，C型慢性肝炎22症例の肝組織を肝生検で採取し，total RNA分画を用いてmicroRNAアレイでmiRNA発現を調べた。その結果，線維化が進行例で発現が高い18個のmiRNAと低下する6個のmiRNAを見いだした。前者の中で$p<0.001$と有意差が高く変動するものはmiR-222，miR-214，miR-199a-3p，miR-199a-5pであり，後者としてはmiR-422aがあった[15]。MurakamiらはC型慢性肝炎の線維化進行度とmiR-199a-3p，miR-199a-5pが相関すると報告していたので[16]，筆者らの報告と一致した。Quantitative RT-PCRを用いて再確認したところ，miR-214，miR-199a-3p，miR-199a-5pとmiR-222に加えてmiR-222のファミリーであるmiR-221はF1-F4へと肝臓の線維化の進行と伴に有意にその発現が上昇することが判明した。また，miR-222とmiR-221の発現は肝組織におけるcollagen 1A1やsmooth muscle α-actin発現とも非常に強い相関があり，これらのmiRNAは肝線維化のよいバイオマーカーになることがわかった。同様の結果は，ヒト非アルコール性脂肪性肝炎でも確認され，また，マウスを用いた肝線維化モデルでも追試された。解析の結果，miR-222とmiR-221は活性化星細胞で高発現すること，その発現にはNF-κBが関与することが明らかとなった。miR-222とmiR-221が線維化肝で上昇する意義については十分には解明できなかったが，miR-222とmiR-221はcyclin-dependent kinase inhibitor 1B(CDKN1B)を制御するため，星細胞あるいは近隣細胞の細胞増殖性シグナルに寄与する可能性が示唆された。

Ⅳ　星細胞増殖におけるcyclin E1とmicroRNA195による制御

前述したように肝線維化病態と星細胞機能制御におけるmiRNAの関与について解析してきたが，その過程でmiR-195がCyclin E1発現において重要であることを見いだした。Cyclin E1はG1サイクリンの一つであるCyclin Eファミリーに属する分子でありcyclin-dependent kinase 2(CDK2)と複合体を形成する。Cyclin E/CDK2複合体は種々の蛋白質のリン酸化を介して細胞増殖を主とする細胞機能の修飾に関与する。すなわち，Cyclin E/CDK2複合体がretinoblastoma protein(Rb)をリン酸化し，それによってE2F転写因子を遊離させ，細胞周期のG1からS phase移行に必要な蛋白質の転写を促進させる。Cyclin E/CDK2複合体はp27やp21をリン酸化することやSmad 3をリン酸化することも示されている。Cyclin E1はそのファミリーの一つであり*CCNE1*遺伝子産物である。

星細胞は活性化されると静止期(quiescent phenotype)から増殖期に移行する。ラットから分離した初代培養星細胞はプラスチックシャーレ上で血清を入れた培養液を用いて培養を継続すると増殖を開始する。筆者らは培養後の時間経過に伴うG0/G1期からS期への移行について詳細に検討したが，星細胞のDNA合成は培養開始後48時間後から開始され，その後S期ならびにG2+M期の細胞が増加することを観察した。それに並行してG1サイクリンであるCyclin D1，Cyclin D2と伴にCyclin Eが増加すること，また，増殖抑制剤であるisobuthylmethylxanthineやdibutyryl cAMPで星細胞を処理すると，これらのG1サイクリンの発現低下がみられることを観察した。以上のことから，初代培養星細胞の増殖にはCyclin Eを含むG1サイクリンが重要であることを示した[17]。

上述したように筆者らは星細胞の活性化の分子機構におけるmiRNAの関与を解析してきたが，miR-195が星細胞の活性化と共に発現低下すること，それと相反してCyclin E1 mRNA発現が著明に低下する($p<0.01$)ことからこの両者に関連

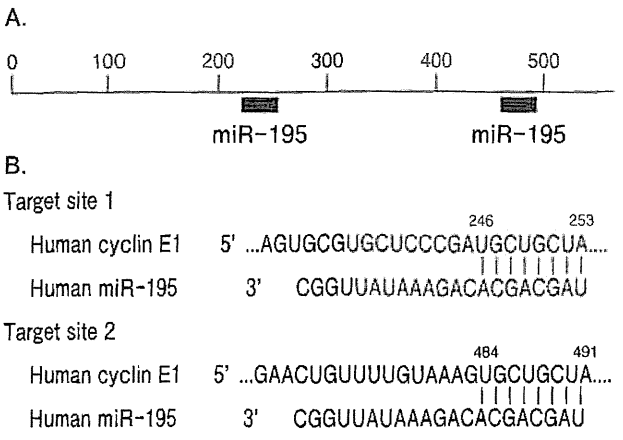

図2 ヒトCyclin E1の3'UTR領域におけるmiR-195の結合部分とその詳細

があるのではないかと推測した。TargetScan (http://www.targetscan.org/)によるとmiR-195はmiR-15abc, 16, 16abc, 322, 424, 497, 1907と共にファミリーを形成し，そのターゲットとしてfibroblast growth fator 2, zinc finger and BTB domain containing 34, importinなどと共にCyclin E1が含まれる。ラット星細胞の細胞株であるLX-2にmiR-195を過剰発現させたところE2F転写因子の発現は影響されなかったが，Cyclin E1 mRNA発現が有意に低下すると同時に，p21 mRNA発現が増加することが判明した。miR-195過剰発現はCyclin E1蛋白質の発現も低下させ，WST-1アッセイによるLX-2細胞の増殖に対しても有意な抑制効果を示した[18]。

TargetScan Human Release 6.2によるとCyclin E1の3' UTR領域には2か所miR-195の結合サイトが存在する(図2)。そこで，この領域をLX-2からクローニングしてルシフェラーゼレポーターベクター(pmirGLO vector)に挿入して，実際にmiR-195がCyclin E1の3' UTR領域に結合するかどうかを確認した。その結果，LX-2においてもmiR-195のCyclin E1の3' UTR領域への結合を確認できた。

以上のことから，miR-195は活性化星細胞では発現低下する。この結果，Cyclin E1の遺伝子発現の抑制が解除され，星細胞でのCyclin E1の増加が生じ，星細胞はG1/S期に移行しやすくなり，その他の蛋白質発現を伴いながら分裂期へと移行する可能性が示唆された。"PubMed"で検索する限りにおいてmiR-195によるCyclin E1発現調節に関する報告はわれわれの報告が初めてであった。

われわれの報告後Huiらはヒトグリオーマ細胞の増殖がmiR-195で制御されることを報告した。すなわち，ヒトグリオーマ細胞株(A172, LN340, U118MGなど)やヒトグリオーマ組織におけるmiR-195発現は正常ヒトアストロサイトや非腫瘍部の脳組織に比較して低下していた。miR-195をLN18あるいはT98Gグリオーマ細胞細胞に過剰発現させるとこれらの細胞増殖は有意に減少することがBrdU取り込みアッセイとフローサイトメトリーによる細胞周期解析で明らかとなった。これらの細胞株にmiR-195を過剰発現させるとCyclin E1やリン酸化CDK2が低下し，逆に，miR-195の阻害剤で処理するとCyclin E1やリン酸化CDK2は増加した。さらにHuiらは*in vivo*においてmiR-195を過剰発現されたLN18細胞はヌードマウスでの移植実験で腫瘍形成が抑制されることを観察した[19]。

V おわりに

ヒトのゲノム解読後，ヒトゲノムの蛋白質をコードしない領域から合成されるRNAの解析が飛躍的に進んだ。miRNAの特徴は一つのmiRNAが一つのmRNAに対応するのではなく，多数の異なるmRNA発現に対して同時に影響を及ぼしうることである。したがって，遺伝子の発現調節機構は従来想像されていたものよりもはるかに複雑であり，その全貌を明らかにする研究はまだ緒についたばかりである。今回の総説ではG1サイクリンの一つであるCyclin E1の発現がmiR-195で調節される可能性を，肝臓の星細胞機能と絡めて概説した。細胞増殖のメカニズムを理解するうえでの一助になることを期待する。

●文 献

1) Bartel DP：*Cell* 136：215-233, 2009
2) Cai X, Hagedorn CH, Cullen BR：*RNA* 10：1957-1966, 2004
3) Winter J, Jung S, Keller S et al：*Nat Cell Biol* 11：228-234, 2009
4) Landgraf P, Rusu M, Sheridan R et al：*Cell* 129：

1401-1414, 2007
5) Shimakami T, Yamane D, Jangra RK et al : *Proc Natl Acad Sci U S A* **109** : 941-846, 2012
6) Janssen HL, Reesink HW, Lawitz EJ at al : *N Engl J Med* **368** : 1685-1694, 2013
7) Huang S, He X : *Br J Cancer* **104** : 235-240, 2011
8) Meng F, Henson R, Wehbe-Janek H et al : *Gastroenterology* **133** : 647-658, 2007
9) Selaru FM, Olaru AV, Kan T et al : *Hepatology* **49** : 1595-1601, 2009
10) Wynn TA, Ramalingam TR : *Nat Med* **18** : 1028-1040, 2012
11) Kawada N : *Hepatol Res* **41** : 199-208, 2011
12) Sekiya Y, Ogawa T, Yoshizato K et al : *Biochem Biophys Res Commun* **412** : 74-79, 2011
13) Kwiecinski M, Elfimova N, Noetel A et al : *Lab Invest* **92** : 978-987, 2012
14) Bandyopadhyay S, Friedman RC, Marquez RT et al : *J Infect Dis* **203** : 1753-1762, 2011
15) Ogawa T, Enomoto M, Fujii H et al : *Gut* **61** : 1600-1609, 2012
16) Murakami Y, Toyoda H, Tanaka M et al : *PLoS One* **6**(1) : e16081, 2011
17) Kawada N, Ikeda K, Seki S at al : *J Hepatol* **30** : 1057-1064, 1999
18) Sekiya Y, Ogawa T, Iizuka M et al : *J Cell Physiol* **226** : 2535-2542, 2011
19) Hui W, Yuntao L, Lun L et al : *PLoS One* **8**(1) : e54932, 2013

次号予告

65巻2号/2014年4月刊

特集　細胞の少数性と多様性に挑む―シングルセルアナリシス

Laboratory Investigation (2014) 94, 192–207

Cytoglobin is expressed in hepatic stellate cells, but not in myofibroblasts, in normal and fibrotic human liver

Hiroyuki Motoyama[1], Tohru Komiya[2], Le Thi Thanh Thuy[1], Akihiro Tamori[1], Masaru Enomoto[1], Hiroyasu Morikawa[1], Shuji Iwai[1], Sawako Uchida-Kobayashi[1], Hideki Fujii[1], Atsushi Hagihara[1], Etsushi Kawamura[1], Yoshiki Murakami[1], Katsutoshi Yoshizato[1,3] and Norifumi Kawada[1]

Cytoglobin (CYGB) is ubiquitously expressed in the cytoplasm of fibroblastic cells in many organs, including hepatic stellate cells. As yet, there is no specific marker with which to distinguish stellate cells from myofibroblasts in the human liver. To investigate whether CYGB can be utilized to distinguish hepatic stellate cells from myofibroblasts in normal and fibrotic human liver, human liver tissues damaged by infection with hepatitis C virus (HCV) and at different stages of fibrosis were obtained by liver biopsy. Immunohistochemistry was performed on histological sections of liver tissues using antibodies against CYGB, cellular retinol-binding protein-1 (CRBP-1), α-smooth muscle actin (α-SMA), thymocyte differentiation antigen 1 (Thy-1), and fibulin-2 (FBLN2). CYGB- and CRBP-1-positive cells were counted around fibrotic portal tracts in histological sections of the samples. The expression of several of the proteins listed above was examined in cultured mouse stellate cells. Quiescent stellate cells, but not portal myofibroblasts, expressed both CYGB and CRBP-1 in normal livers. In fibrotic and cirrhotic livers, stellate cells expressed both CYGB and α-SMA, whereas myofibroblasts around the portal vein expressed α-SMA, Thy-1, and FBLN2, but not CYGB. Development of the fibrotic stage was positively correlated with increases in Sirius red-stained, α-SMA-positive, and Thy-1-positive areas, whereas the number of CYGB- and CRBP-1-positive cells decreased with fibrosis development. Primary cultured mouse stellate cells expressed cytoplasmic CYGB at day 1, whereas they began to express α-SMA at the cellular margins at day 4. Thy-1 was undetectable throughout the culture period. In human liver tissues, quiescent stellate cells are CYGB positive. When activated, they also become α-SMA positive; however, they are negative for Thy-1 and FBLN2. Thus, CYGB is a useful marker with which to distinguish stellate cells from portal myofibroblasts in the damaged human liver.
Laboratory Investigation (2014) **94,** 192–207; doi:10.1038/labinvest.2013.135; published online 2 December 2013

KEYWORDS: α-smooth muscle actin; cellular retinol binding protein-1; chronic hepatitis; cytoglobin; fibulin-2; Thy-1

Stellate cell activation-associated protein was originally discovered by proteomic analysis (in 2001)[1] in cultured rat hepatic stellate cells that have vitamin A storage ability when quiescent and function as liver-specific pericytes. Histoglobin[2] and Cytoglobin (CYGB)[3] were reported by Trent and Hargrove[2] and by Burmester *et al*,[3] respectively, in 2002. These proteins, in addition to stellate cell activation-associated protein, were classified as human, mouse, and rat homologs of a hexacoordinate globin that differs from the traditional pentacoordinate globins, such as myoglobin and hemoglobin.[4] CYGB consists of 190 amino acids with a calculated molecular mass of 21 kDa, and its amino acid sequence is highly conserved among species.[3] Human CYGB has ~25% amino acid identity with vertebrate myoglobin and hemoglobin and 16% identity with human neuroglobin, which is another type of globin that is present specifically in the nervous system. CYGB is thus recognized as the fourth globin of mammals.[5] The *CYGB* gene is located on human chromosome 17q25.3 and mouse chromosome 11E2.

Although myoglobin, hemoglobin, and neuroglobin are tissue restricted to cardiomyocytes and skeletal myofibers, erythrocytes, and the nervous system, respectively, CYGB is ubiquitously expressed in the cytoplasm of mesenchymal fibroblastic cells of many organs,[6] and CYGB was reported to

[1]Department of Hepatology, Graduate School of Medicine, Osaka City University, Osaka, Japan; [2]Department of Biological Function, Faculty of Science, Osaka City University, Osaka, Japan and [3]PhoenixBio, Higashihiroshima, Hiroshima, Japan
Correspondence: Dr N Kawada, MD, PhD, Department of Hepatology, Graduate School of Medicine, Osaka City University, 1-4-3 Asahimachi, Abeno, Osaka 545-8585, Japan.
E-mail: kawadanori@med.osaka-cu.ac.jp
Received 26 April 2013; revised 20 September 2013; accepted 4 October 2013

be present in the nucleus of human hepatocytes.[7] In particular, CYGB is present in stellate cells in the liver and pancreas, reticulocytes in the spleen, mesenchymal cells in the submucosal layer of the gut, and mesangium cells and stromal cells in the rat kidney. Therefore, one interesting aspect of CYGB expression is its presence in visceral cells that have the ability to store vitamin A. CYGB has also been observed in some neuronal subpopulations of the central and peripheral nervous systems in humans.

Hepatic stellate cells have conventionally been recognized as hepatic fibroblastic cells (myofibroblasts are also categorized as this cell type) that preferentially localize to the portal region. Considering that quiescent stellate cells are transformed into activated stellate cells, the liver contains at least three types of fibroblastic cells: stellate cells, activated stellate cells, and portal myofibroblasts.[8,9] Stellate cells are desmin positive in rodents[10] and, when activated, they express α-smooth muscle actin (α-SMA). In addition, these cells express cellular retinol-binding protein-1 (CRBP-1) and participate in the metabolism of retinol and retinyl esters.[11] In contrast, thymocyte differentiation antigen 1 (Thy-1 or CD90)[12–14] and fibulin-2 (FBLN2)[15–17] have been utilized as markers of liver myofibroblasts. These cell type-specific markers of liver fibroblastic cells have been largely utilized in studies with rodents. However, a specific marker to distinguish stellate cells from myofibroblasts in the human liver has not yet been identified.

The aims of our present work were to investigate whether CYGB is a reliable marker of stellate cells in the normal human liver and to study the expression of CYGB, CRBP-1, Thy-1, FBLN2, and α-SMA in fibrotic and cirrhotic human liver.

MATERIALS AND METHODS

Human Liver Tissues

Human liver tissues damaged by hepatitis C virus (HCV) infection at various fibrosis stages (from F1 to F4, 10 samples each) and one tissue sample damaged by nonalcoholic steatohepatitis (NASH) at fibrosis stage F2 (58-year-old woman with serum alanine aminotransferase (ALT) 110 IU/l) were obtained by liver biopsy at Osaka City University Medical School Hospital (Osaka, Japan) from August 2006 to September 2011. Intact human liver tissues were obtained from patients who had metastatic liver tumors or cholangiocarcinoma treated by surgical resection. The procedures for this study were in accordance with the Helsinki Declaration of 1975 (2000 revision). Liver biopsy was performed after informed consent had been granted.

Clinical Data

The age, sex, and primary clinical data for each patient were obtained on consultation or admission to our university hospital. ALT levels, albumin levels, platelet counts, and anti-HCV antibody levels were measured at the Central Clinical Laboratory of Osaka City University Medical School Hospital (Table 1).

Table 1 Characteristics of the HCV-infected patients enrolled in this study

Stage	Age[a] (years)	ALT[b] (IU/l)	Albumin[a] (g/dl)	Platelet[a] ($\times 10^3$/mm^3)	Grade (A0/A1/A2/A3)
F1	55.5 ± 13.7	63.5 (25.0–89.0)	4.1 ± 0.3	17.9 ± 5.4	3/7/0/0
F2	55.6 ± 8.7	60.2 (40.5–74.0)	3.9 ± 0.3	15.0 ± 5.4	0/5/5/0
F3	63.8 ± 8.1	75.1 (48.2–103.5)	3.8 ± 0.3	12.6 ± 3.2	0/2/5/3
F4	63.0 ± 6.8	82.4 (44.7–115.2)	3.6 ± 0.3	12.0 ± 4.1	0/4/6/0

ALT, alanine aminotransferase.
The stage of liver fibrosis and grade of necroinflammation were assessed based on the new Inuyama classification.[19]
[a]Mean ± s.d.
[b]Median (interquartile range).

Histopathological Diagnosis

Liver biopsy was performed in all 41 patients using a 15-gauge Tru-Cut needle (Hakko, Tokyo, Japan) under ultrasound guidance. The tissue samples fulfilled the size requirements suggested by Janiec *et al*:[18] adequate liver biopsy samples were defined as having a length > 1.0 cm and/or the presence of at least 10 portal tracts. The liver tissues were fixed in 10% formaldehyde, embedded in paraffin, and cut into 4-μm-thick sections. Deparaffinized sections were stained with hematoxylin–eosin and Azan–Mallory, dehydrated in 100% ethanol, cleared by xylene, mounted with NEW M·X (Matsunami Glass Industries, Osaka, Japan), and then examined by microscopy. The degree of liver fibrosis was assessed based on the new Inuyama classification[19] as follows: F0, no fibrosis; F1, expansion of the portal tracts without linkage; F2, portal expansion with portal-to-portal linkage; F3, extensive portal-to-portal and focal portal-to-central linkage; and F4, cirrhosis (Table 1).

The sections were also stained with 0.1% (w/v) Sirius red (Direct Red 80; Aldrich, Milwaukee, WI, USA) in a saturated aqueous picric acid solution for 1 h at room temperature to visualize collagen fibers. After staining, the sections were washed in two changes of 0.01 N HCl and mounted as described above.[20]

Immunostaining of Human Liver Tissues

For immunohistochemistry, paraffin sections were dewaxed in xylene and rehydrated in decreasing concentrations of ethanol (xylene: 3 × 3 min; 100% ethanol: 2 × 3 min; 95% ethanol: 3 min; 70% ethanol: 3 min). Primary antibodies and immunohistochemistry conditions are listed in Table 2. In brief, the sections were deparaffinized and treated with a solution of 3% H_2O_2 in 100% methanol for 10 min at room temperature to block endogenous peroxidase activity.

Table 2 Primary antibodies used in this study

Antibody	Species	Source	Dilution
Anti-human cytoglobin	Rb poly	Our laboratory	1/100
Anti-human cytoglobin	Mo mono	Our laboratory	1/1000
Anti-rat cytoglobin	Rb poly	Our laboratory	1/100
Anti-human cellular retinol-binding protein-1	Rb poly	Santa Cruz	1/100
Anti-human α-smooth muscle actin	Mo mono	Dako	1/100
Anti-human thymocyte differentiation antigen 1 (Thy-1)	Rb poly	Abcam	1/100
Anti-mouse thymocyte differentiation antigen 1 (Thy-1)	Mo mono	Abcam	1/100
Anti-human fibulin-2 (FBLN2)	Rb poly	Sigma	1/200
Anti-human lymphatic vessel endothelial hyaluronan receptor-1 (LYVE-1)	Rb poly	Abcam	1/200

Mo mono, mouse monoclonal antibody; Rb poly, rabbit polyclonal antibody.

The sections were then preincubated with serum-free protein block (Dako, Glostrup, Denmark) for 10 min at room temperature and subsequently incubated with primary antibodies in a dilution of 1:100 for 1 h at room temperature. Negative controls with no primary antibody were used to assess nonspecific staining. The secondary antibodies used included horseradish peroxidase-conjugated goat anti-rabbit IgG (1:200; Dako), rabbit anti-goat IgG (1:200; Dako), and rabbit anti-mouse IgG (1:200; Dako). The chromogen used was 3,3′-diaminobenzidine (Dako). The resultant sections were stained and analyzed using a BZ-8000 microscope (Keyence, Osaka, Japan).

Subsequently, double immunofluorescence staining was performed. After the paraffin sections were dewaxed, the sections were incubated with a mixture of antibodies against CYGB and α-SMA as described previously.[21] After rinsing in PBS, the sections were incubated with a mixture of fluorochrome-conjugated secondary antibodies: AlexaFluor 488 goat anti-rabbit IgG (Molecular Probes, Eugene, OR, USA) and AlexaFluor 594 goat anti-mouse IgG (Molecular Probes). The sections were briefly washed and mounted with ProLong Gold Antifade Reagent (Molecular Probes). The resulting sections were stained and analyzed using a BZ-8000 microscope (Keyence).

Morphometry for Hepatic Fibrosis

For morphometric image analysis of hepatic fibrosis in immunostaining, the areas of the liver sections that were positive for Sirius red (red), α-SMA (brown), or Thy-1 (brown) were captured separately using a charge-coupled device (CCD) camera connected to a macro digital filing system (DP70 · BX-51; Olympus Corporation, Tokyo, Japan). Images representing the whole biopsy section were acquired at × 200 magnification and digitalized. These separately captured and digitalized images were consolidated to create one large image using e-Tiling (Mitani Corporation, Tokyo, Japan). Collagen- or α-SMA-positive areas were measured using Lumina Vision 2.4 (Mitani Corporation) and were calculated automatically. The hepatic fibrotic area (%) was calculated as the area stained with the selected color divided by the whole tissue area at × 100 magnification.[20]

In fibrotic livers, the number of CYGB- and CRBP-1-positive stellate cells in each field was counted around fibrotic portal tracts (F1 to F4 samples). The analysis was performed on each 10-sample group of F1–F4 tissues using an average of five fields per zone (1.4 mm^2) (100 × objective). We counted the cell bodies that stained positively and contained a nucleus.

Cell Lines

The human HSC line LX-2 was donated by Dr Scott L Friedman at the Mount Sinai School of Medicine (New York, NY, USA).[22] LX-2 cells were cultured on plastic dishes or glass chamber slides in Dulbecco's modified Eagle's medium (DMEM; Sigma Chemical, St Louis, MO, USA) supplemented with 10% fetal bovine serum (FBS; Invitrogen, Carlsbad, CA, USA), 100 U/ml penicillin, and 100 μg/ml streptomycin. Huh7 cells (JCRB0403), which were obtained from the Japanese Collection of Research Bioresources (JCRB) Cell Bank (Osaka, Japan), were maintained on plastic culture plates in DMEM supplemented with 10% FBS. In some experiments, LX-2 cells were transfected with the pEGFP-cytoglobin vector (Clontech, Mountain View, CA, USA) using FuGENE HD (Roche, Applied Science, Indianapolis, IN, USA). The cells were collected at 24 h after transfection.

Preparation of Primary Cultured Mouse Hepatic Stellate Cells

Primary mouse stellate cells were isolated from 12- to 16-week-old male C57BL/6N mice (Japan SLC, Shizuoka, Japan) by pronase–collagenase digestion and subsequent purification with a single-step Nycodenz gradient, as previously described.[23] All animals received humane care. The experimental protocol was approved by the Committee

of Laboratory Animals, Osaka City University Medical School, and was performed according to institutional guidelines. Isolated stellate cells were cultured on plastic dishes or glass chamber slides in DMEM (Sigma Chemical) supplemented with 10% FBS (Invitrogen), 100 U/ml penicillin, and 100 μg/ml streptomycin. The purity of the cultures was determined based on observation of the characteristic stellate cell shape using phase-contrast microscopy.

Quantitative Real-Time PCR

Total RNA was extracted from stellate cells using the RNeasy Mini Kit (Qiagen, Valencia, CA, USA). cDNA was synthesized as previously described.[24] Gene expression was measured by quantitative real-time PCR using cDNA, THUNDERBIRD SYBR qPCR Mix Reagents (Toyobo, Osaka, Japan), and a set of gene-specific oligonucleotide primers. The reactions were performed in an Applied Biosystems Prism 7500 Sequence Detection System (Applied Biosystems, Foster City, CA, USA). The expression of glyceraldehyde-3-phosphate dehydrogenase (GAPDH) was also measured as an internal control.

Immunoblotting

Protein samples (30 μg) were subjected to 5–20% gradient SDS-polyacrylamide gel electrophoresis (ATTO, Tokyo, Japan) and transferred to Immobilon P membranes (Millipore Corporation, Bedford, MA, USA). After blocking, the membranes were probed with a primary antibody against CYGB (1:1000; our laboratory), α-SMA (1:2000; Dako), Thy-1 (1:1000; Abcam, Cambridge, UK), or GAPDH (1:2000; Santa Cruz Biotechnology, Santa Cruz, CA, USA). The membranes were then labeled with horseradish peroxidase-conjugated secondary antibodies. Immunoreactive bands were visualized using the ECL detection reagent (GE Healthcare, Buckinghamshire, UK) and documented with an LAS 1000 device (Fuji Photo Film, Kanagawa, Japan).

Data Analysis

The data are presented as bar graphs representing the mean ± s.d. in all experiments. Statistical analyses were performed using Student's *t*-test. $P<0.05$ indicated statistical significance.

RESULTS

Specificity of the Anti-CYGB Antibody

We previously generated rabbit polyclonal anti-rat CYGB antibodies that stain stellate cells in intact and fibrotic rat liver and other visceral organs.[1,25] In the present study, we newly generated rabbit polyclonal and mouse monoclonal antibodies against human CYGB in our laboratory. Immunoblot analysis revealed that the rabbit polyclonal antibodies detected purified recombinant human CYGB,[26] which was provided by RIKEN (Harima, Hyogo, Japan), at 21 kDa and EGFP-binding recombinant human CYGB (generated in our laboratory) at 48 kDa; however, the antibodies did not detect human albumin. LX-2 and Huh 7 cells expressed negligible levels of CYGB (Figure 1a). The monoclonal antibody produced almost identical results (data not shown).

Immunohistochemical Characterization of Intact Human Liver

Intact human liver tissues were obtained by surgical resection from patients with metastatic liver tumors or cholangiocarcinoma, and the expression levels of CYGB, α-SMA, Thy-1, and FBLN2 were determined (Figure 1). As shown in Figure 1bA and B, the obtained tissue samples showed negligible inflammatory cell infiltration and negligible expansion of fibrotic areas. Immunostaining using the polyclonal antibodies against human CYGB revealed positive cells along the sinusoids throughout the lobule (Figure 1bC and D). Similar results were obtained with the monoclonal antibody (Figure 1bE and F). The hepatocytes and the cells in the portal areas were CYGB negative. CYGB-positive cells were present in the serial sections, and we identified these cells as stellate cells because an enlarged view revealed that they were located between the hepatocytes and the lumen of the sinusoids. In addition, these cells contained lipid droplets in their cytoplasm, and their cytoplasmic processes expanded along the sinusoids (Figure 1bD and F).

Immunohistochemistry was further performed on intact human liver samples using antibodies against CRBP-1, α-SMA, FBLN2, and Thy-1. In the liver parenchyma, strong expression of CRBP-1 was observed along the sinusoids (Figure 2a). An enlarged view showed that CRBP-1-positive cells contained lipid droplets, indicating that they were hepatic stellate cells. There were no CRBP-1-positive cells around the portal area. Instead, α-SMA-positive cells predominated; these cells also existed in the walls of the vessels, but not along the hepatic sinusoids (Figure 2b). In addition, the regions adjacent to the portal vein contained limited numbers of cells that stained for FBLN2 or Thy-1 (Figure 2c and d), which are also biomarkers of myofibroblasts.

Taken together, these findings indicate that CYGB and CRBP-1 are uniquely expressed in hepatic stellate cells in the intact human liver, whereas myofibroblast markers such as α-SMA, FBLN2, and Thy-1 are locally present in cells around the portal tract.

Immunohistochemistry of CD68, LYVE-1, and CRBP-1 in Relation to CYGB

CD68 is a glycoprotein that binds to low-density lipoprotein and is expressed by monocytes and macrophages. Kupffer cells are positive for CD68.[27] We found that spindle-shaped CD68-positive cells were present in the sinusoids in the intact human liver, indicating that these cells were Kupffer cells. These cells were predominantly located along the sinusoids (Figure 3a). Double immunofluorescence staining

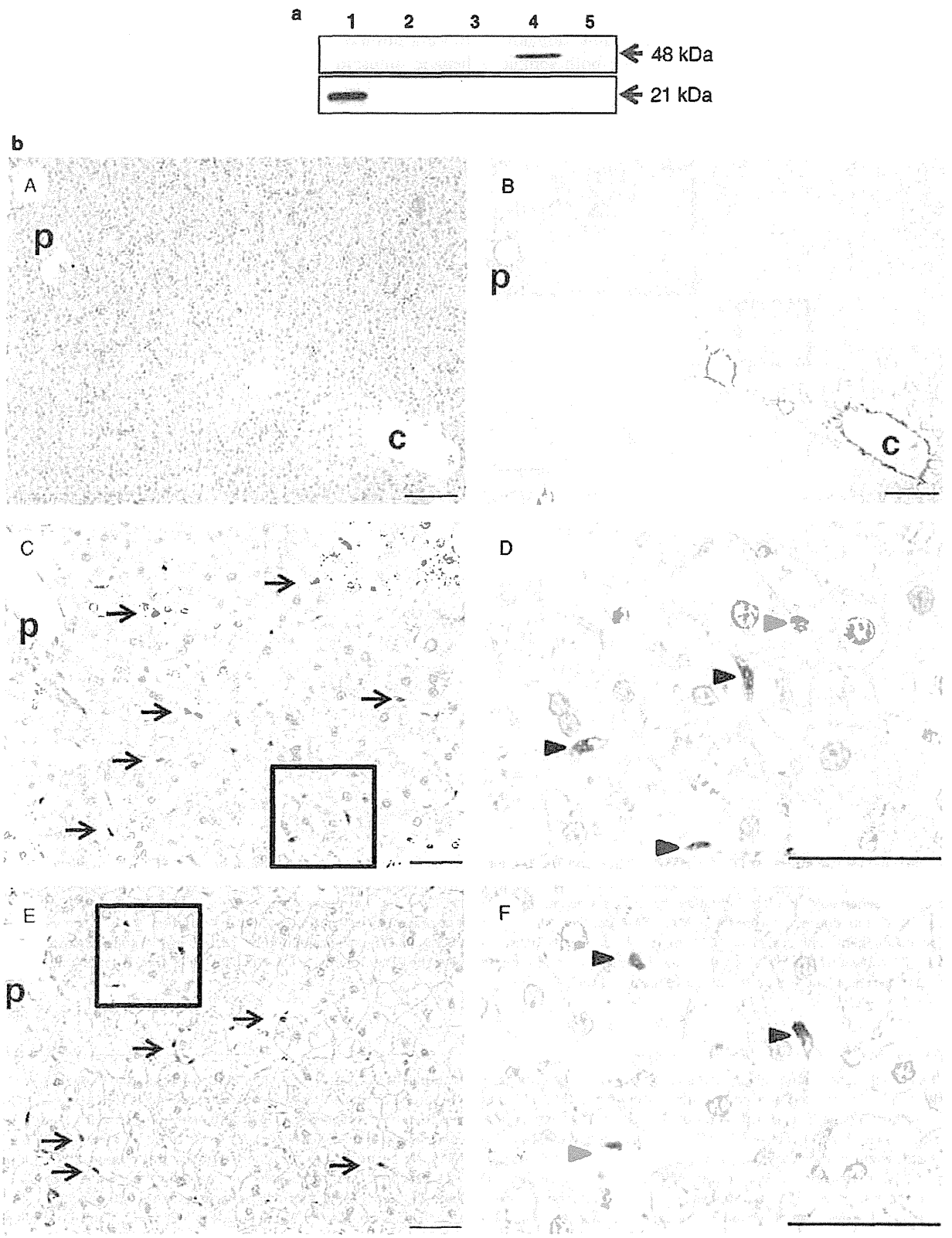
a
1
2
3
4
5
48 kDa
21 kDa
b
A
p
c
B
p
c
C
p
D
E
p
F

showed that CD68 did not colocalize with CYGB (Figure 3b–d). LYVE-1, also known as extracellular link domain-containing 1 (XLKD1), acts as a receptor for both soluble and immobilized hyaluronan. Sinusoidal endothelial cells are LYVE-1 positive.[28] We observed LYVE-1 positivity along the hepatic sinusoid in the sinusoidal walls, indicating that

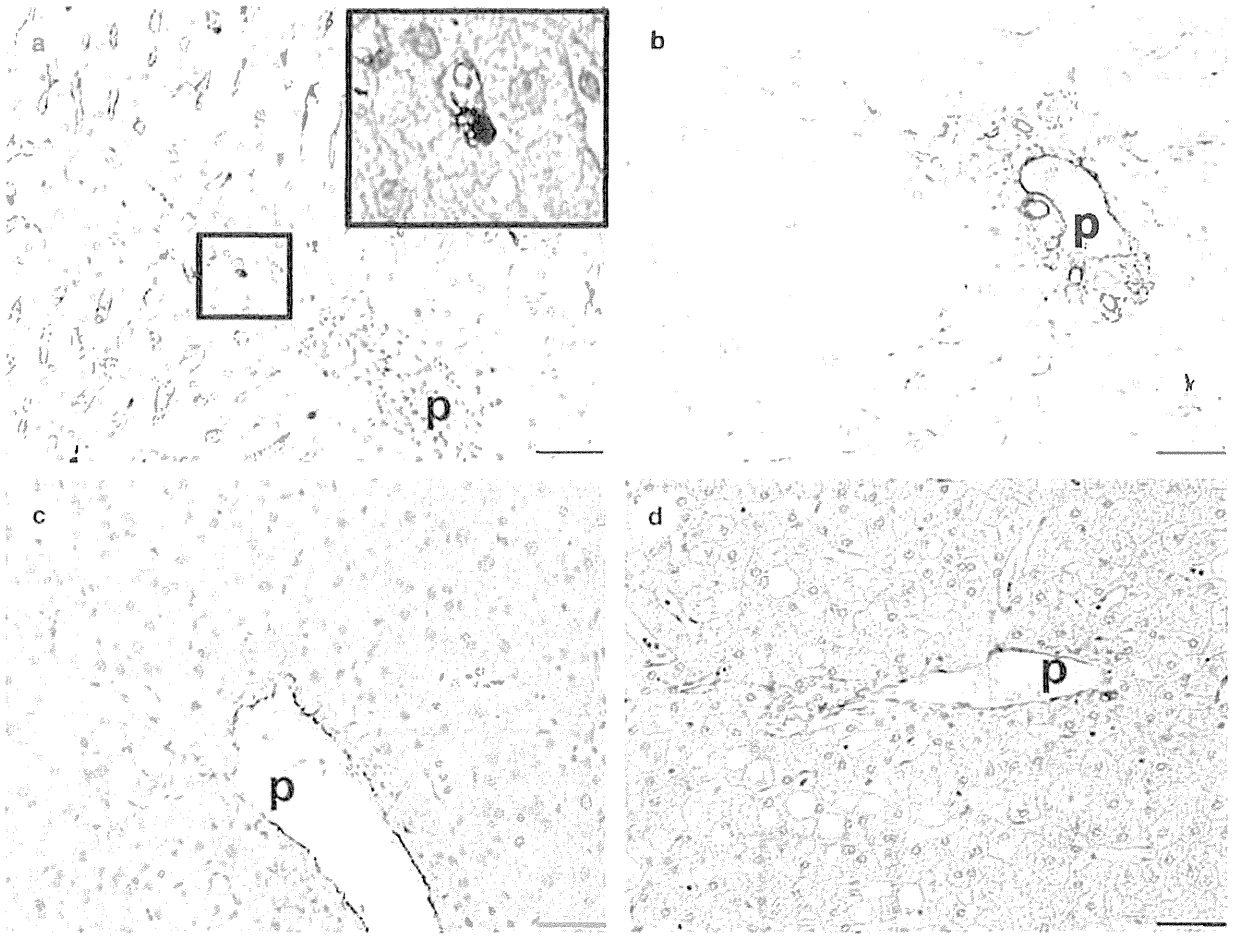

Figure 2 Immunohistochemistry for CRBP-1, α-SMA, FBLN2, and Thy-1 in intact human liver. (**a**) Immunohistochemistry for CRBP-1. In the liver parenchyma, strong expression of CRBP-1 was observed along the sinusoids (arrows). A magnified view of the enclosed area shows that a CRBP-1-positive cell contained lipid droplets, indicating that it was a hepatic stellate cell. CRBP-1 was not observed around the portal area. Bar, 100 μm. p, portal vein. (**b**) Immunohistochemistry for α-SMA. α-SMA-positive cells were present predominantly in the portal area and in the walls of the vessels, but not along the hepatic sinusoids. Bar, 100 μm. (**c**) Immunohistochemistry for FBLN2. FBLN2 was localized in the vessels of the portal spaces. Positive staining for FBLN2 was not visible along the sinusoids. Bar, 100 μm. (**d**) Immunohistochemistry for Thy-1. Thy-1-positive cells were located within the portal tracts adjacent to the wall of the portal vein. Bar, 100 μm.

Figure 1 Characterization of newly generated rabbit polyclonal antibodies against human CYGB. (**a**) Newly generated rabbit polyclonal antibodies against human CYGB detected purified recombinant human CYGB (21 kDa) (lane 1) and EGFP-labeled recombinant human Cygb (48 kDa) (lane 4) but not human albumin (lane 2). LX-2 cells and Huh 7 cells did not express CYGB (lanes 3 and 5, respectively). (1) Recombinant human CYGB (10 μg); (2) human albumin (20 μg); (3) lysate of LX-2 cells (20 μg); (4) lysate of LX-2 cells overexpressing EGFP-CYGB (20 μg); (5) lysate of Huh-7 cells (20 μg). (**b**) Immunohistochemistry of normal human liver tissues. (A) Hematoxylin–eosin staining. No hepatocyte death or inflammation was observed. Bar, 100 μm. c, central vein; p, portal vein. (B) Sirius red staining. Limited collagen deposition was observed around the portal and central vein areas. No fibrosis occurred in the liver parenchyma. Bar, 100 μm. (C) Immunohistochemistry for CYGB using newly generated polyclonal antibodies. CYGB-positive cells were localized in the liver parenchyma along hepatic sinusoids (arrows). Bar, 100 μm. (D) Magnified view of the enclosed area in (C). CYGB-positive cells were present in the perisinusoidal space and contained lipid droplets in the cytoplasm, suggesting that they were stellate cells (arrowheads). Bar, 20 μm. (E) Immunohistochemistry for CYGB using the monoclonal antibody. CYGB-positive cells were localized in the liver parenchyma along the hepatic sinusoids (arrows). Bar, 100 μm. (F) Magnified view of the enclosed area in (E). CYGB-positive cells were present in the perisinusoidal space and contained lipid droplets in the cytoplasm, suggesting that they were stellate cells (arrowheads). Bar, 20 μm.

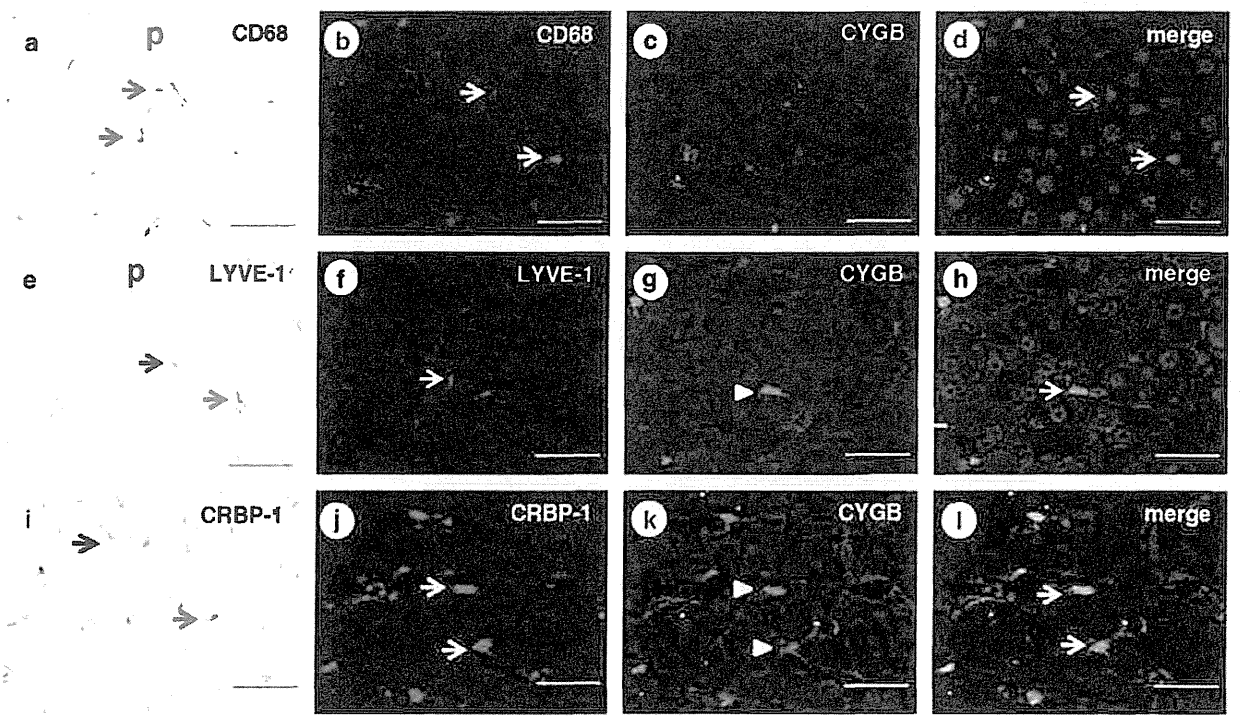

Figure 3 Immunohistochemistry for CD68, LYVE-1, and CRBP-1 in the intact human liver. (**a–d**) Immunohistochemistry for CD68 and CYGB. CD68-positive cells (arrows) were located inside the sinusoidal lumen (**a**). Double immunofluorescence showed that CYGB (**b**) and CD68 (c) did not colocalize as shown in panel **d**. p, portal vein. Bar, 100 μm. (**e–h**) Immunohistochemistry for LYVE-1 and CYGB. LYVE-1-positive cells (arrows) were localized along the hepatic sinusoids (**e**). Double immunofluorescence showed that LYVE-1 (**f**) and CYGB (**g**, arrowhead) did not colocalize, as shown in (**h**). Bar, 100 μm. (**i–l**) Immunohistochemistry for CRBP-1 and CYGB. CRBP-1-positive cells (arrows) were localized in the perisinusoidal space (**i**). Double immunofluorescence showed that CRBP-1 (**j**) and CYGB (**k**, arrowheads) were entirely colocalized, as shown in (**l**). Bar, 100 μm.

LYVE-1-positive cells are sinusoidal endothelial cells in the intact human liver (Figure 3e). Double immunofluorescence staining showed that LYVE-1 did not colocalize with CYGB (Figure 3f–h). Therefore, CYGB was not expressed in hepatocytes, Kupffer cells, or sinusoidal endothelial cells. Double immunostaining for CRBP-1 (Figure 2a and Figure 3i) and CYGB (Figure 3j–l) supported the notion that normal liver tissues contain CYGB- and CRBP-1-double-positive quiescent stellate cells.

CYGB Expression in Fibrotic and Cirrhotic Human Livers

Liver tissues were isolated from patients at different HCV-induced fibrosis stages (from F1 to F4) and subjected to histochemical and immunohistological examination (Figure 4). The extent of collagen deposition at each fibrosis stage was estimated by Sirius red staining, which is shown in Figure 4aA (for F1), E (F2), I (F3), and M (F4). In the liver parenchyma, cells that were positive for CYGB (Figure 4 B, F, J, and N) or CRBP-1 (Figure 4C, G, K, and O) were present along the hepatic sinusoids, indicating that they were stellate cells. α-SMA was expressed in cells around the periportal area, and its expression extended along the expansion of collagen deposition, as shown by Sirius red staining, and along the hepatic sinusoids (Figure 4 D, H, L, and P). Notably, CYGB- and CRBP-1-positive cells (stellate cells) were present inside the hepatic nodules; however, they were scarce in the fibrotic septum of cirrhotic (F4) livers (Figure 4N for CYGB and Figure 4O for CRBP-1), in contrast with the abundance of α-SMA-positive cells in the fibrotic septum (Figure 4P). We further studied the expression of CYGB, CRBP-1, and α-SMA in human NASH tissue (fibrosis stage F2). The results were similar to those obtained in HCV-induced fibrotic tissue: CYGB- and CRBP-1-positive cells were present along the hepatic sinusoids in the liver parenchyma, and α-SMA was expressed by cells around the portal area, with its expression extending along the deposited collagen (Figure 4Q, R, and S).

To quantify the immunohistochemistry results, we performed immunoblot analysis using rabbit polyclonal anti-human CYGB antibodies, which specifically react with human CYGB but not mouse CYGB, in human liver samples and fibrotic mouse livers. We detected a band at the position of purified recombinant human CYGB (21 kDa) in HCV-infected human fibrotic liver tissues at the F2 stage; however, this band was not detected in normal human liver samples. In addition, no CYGB band was observed in fibrotic liver tissues from mice treated with a choline-deficient amino acid-defined diet (for 32 weeks) or *N,N*-diethylnitrosamine

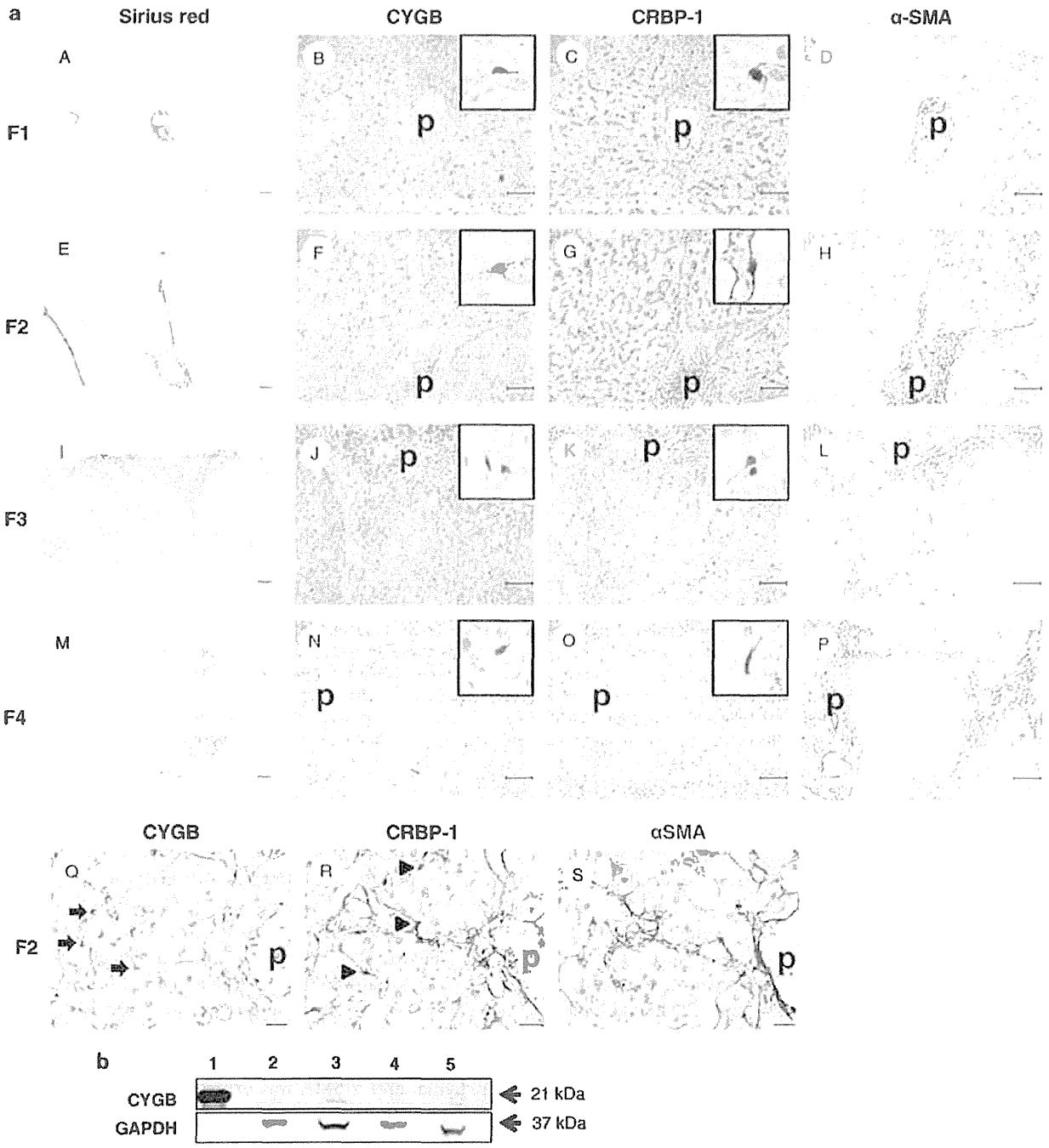

Figure 4 (**a**) Histological analyses of human liver fibrosis at different stages (F1 to F4) according to the new Inuyama classification. (A, E, I, M) Sirius red staining. Bar, 50 μm. (B, F, J, N, Q) Immunohistochemistry for CYGB. Bar, 50 μm. Inserts show high-magnification views of CYGB-positive cells in the liver parenchyma. (C, G, K, O, R) Immunohistochemistry for CRBP-1. Bar, 50 μm. Inserts show high-magnification views of CRBP-1-positive cells in the liver parenchyma. (D, H, L, P, S) Immunohistochemistry for α-SMA. Bar, 50 μm. p, portal vein. (**b**) Immunoblot analysis using rabbit polyclonal anti-human CYGB antibodies that specifically react with human CYGB but not mouse CYGB, with human liver samples and fibrotic mouse livers. (1) Recombinant human CYGB (10 μg); (2) normal human liver (25 μg); (3) hepatitis C virus-infected human liver (25 μg); (4) fibrotic liver from a mouse treated with a choline-deficient amino acid-defined diet (25 μg); and (5) fibrotic liver from a mouse treated with *N,N*-diethylnitrosamine (25 μg). Note that this analysis also revealed the induction of CYGB in fibrotic human livers.

(25 p.p.m. for 25 weeks). Thus, this analysis also revealed the induction of CYGB in fibrotic human livers (Figure 4b).

The scarcity of CYGB- and CRBP-1-positive cells in the fibrotic septum is convincingly shown in Figure 5. The distribution patterns of three myofibroblast biomarkers, α-SMA (Figure 5b, e, h, k, n), Thy-1 (Figure 5c, f, i, and l), and FBLN2 (Figure 5o), in the portal areas were nearly identical in fibrotic livers. The distribution of CYGB was mutually exclusive with the distribution of these three proteins (Figure 5a, d, g, j, and m).

The mutually exclusive localization patterns of these cell type-specific markers were further examined by double immunofluorescence staining (Figure 6). CYGB was expressed in cells close to the parenchymal area of F1 to F3 livers (Figure 6a, d, and g), and its expression did not overlap with that of α-SMA (Figure 6c, f, and i). However, in the F4 liver, cells near the extended fibrotic septum were double positive for CYGB and α-SMA, strongly suggesting that these cells were activated stellate cells. In the F3 liver, neither FBLN2 nor Thy-1 overlapped with CYGB (Figure 6m–r).

Taken together, these data reveal that CYGB and CRBP-1 are excellent markers of human stellate cells in both intact and fibrotic livers and that stellate cells become positive for α-SMA when activated. We hypothesize that cells positive for FBLN2 and Thy-1 are different from stellate cells and exhibit the phenotype of portal myofibroblasts that are α-SMA positive in intact human liver tissue.

Quantitative Analysis of the Contributions of Stellate Cells and Myofibroblasts to the Progression of Fibrosis

Of the 40 HCV-infected patients who underwent liver biopsy, the proportion of fibrotic area (as determined by Sirius red staining and immunostaining for α-SMA and Thy-1) was significantly correlated with the stage of liver fibrosis according to the new Inuyama classification. The Sirius red-positive area increased from 1.8% in F1 to 3.66%, 8.57%, and 16.8% in F2, F3, and F4, respectively (Figure 7a). Similarly, the α-SMA-positive area increased from 1.26% in F1 to 1.82%, 5.65%, and 8.31% in F2, F3, and F4, respectively (Figure 7b). The Thy-1-positive area increased from 1.13% in F1 to 2.13%, 5.43%, and 7.52% in F2, F3, and F4, respectively (Figure 7c). In contrast, the density of CYGB-positive cells (Figure 7d) and CRBP-1-positive cells (Figure 7e) was inversely correlated with the progression of liver fibrosis; the density of CYGB-positive cells was 17.9 ± 1.29, 19.7 ± 1.01, 16.2 ± 0.82, and 13.8 ± 1.06 cells/mm^2 in F1, F2, F3, and F4, respectively, and the density of CRBP-1-positive cells was 9.56 ± 1.24, 14.6 ± 0.77, 12.1 ± 0.83, and 9 ± 0.67 cells/mm^2 in F1, F2, F3, and F4, respectively.

CYGB Expression in Primary Mouse Stellate Cells

We determined above the *in vivo* expression profiles of cell type-specific biomarkers in stellate cells and myofibroblasts in intact and fibrotic human liver tissues. Next, we questioned whether these *in vivo* expression profiles could be reproduced in an *in vitro* system. We utilized primary cultures of mouse stellate cells rather than human stellate cells because human stellate cells in a normal quiescent stage are difficult to obtain for laboratory use. These cells were cultured for up to 7 days, during which changes in the expression levels of CYGB, α-SMA, and Thy-1 were immunohistochemically examined (Figure 8).

At 1 day of culture after isolation from the intact liver, mouse stellate cells adhered to plastic plates and exhibited round cell bodies with numerous lipid droplets similar to those observed in lipocytes (Figure 8aA). The cell bodies then began to gradually spread and flatten, and they successively increased in size and lost their lipid droplets, resulting in an activated myofibroblastic phenotype (Figure 8aB and C). Immunocytochemical analyses confirmed the consistent expression of CYGB until day 7 of culture (Figure 8aA–C). α-SMA was not observed at day 1 (Figure 8aD); however, it later appeared at days 4 and 7 (Figure 8aE and F). Double immunofluorescence analysis confirmed the presence of both CYGB and α-SMA in stellate cells at days 4 and 7 (Figure 8aH and J), although their intracellular localization patterns were different; Cygb was distributed diffusely in the cytoplasm, whereas α-SMA tended to accumulate at the periphery of the cells. Immunostaining for CRBP-1 and α-SMA yielded similar results, although CRBP-1 expression was decreased in 7-day-cultured stellate cells, presumably because of the loss of vitamin A in the cytoplasm (data not shown). Thy-1 was not observed throughout the culture period (Figure 8aM–O). The above-mentioned expression profiles of the marker proteins were confirmed by immunoblot analysis (Figure 8b). These results led us to hypothesize that the α-SMA-positive cells observed at later stages of culture were not myofibroblasts but rather activated stellate cells because they were Thy-1 negative.

DISCUSSION

Cytoglobin Is an Excellent Marker of Human Stellate Cells

CYGB was previously isolated from cultured rat hepatic stellate cells that have vitamin A storage ability in the quiescent state and function as liver-specific pericytes.[1]

Figure 5 Histological analyses of human liver fibrosis at different stages (F1 to F4) according to the new Inuyama classification. Immunohistochemistry for CYGB (**a**, **d**, **g**, **j**, **m**), α-SMA (**b**, **e**, **h**, **k**, **n**), Thy-1 (**c**, **f**, **i**, **l**), and FBLN2 (**o**). At each stage, CYGB (arrows) had limited expression in sinusoids, and the positive cells were deemed stellate cells. α-SMA was expressed in the vessel walls of the portal vein and artery, around bile ducts, and in the cells in Glisson's capsule. Some α-SMA-positive cells were also present in the parenchyma at stage F4 (**k**). Both Thy-1 and FBLN2 had limited expression in Glisson's capsule and the extended fibrotic septum in all stages of liver fibrosis. Bar, 50 μm. p, portal vein.

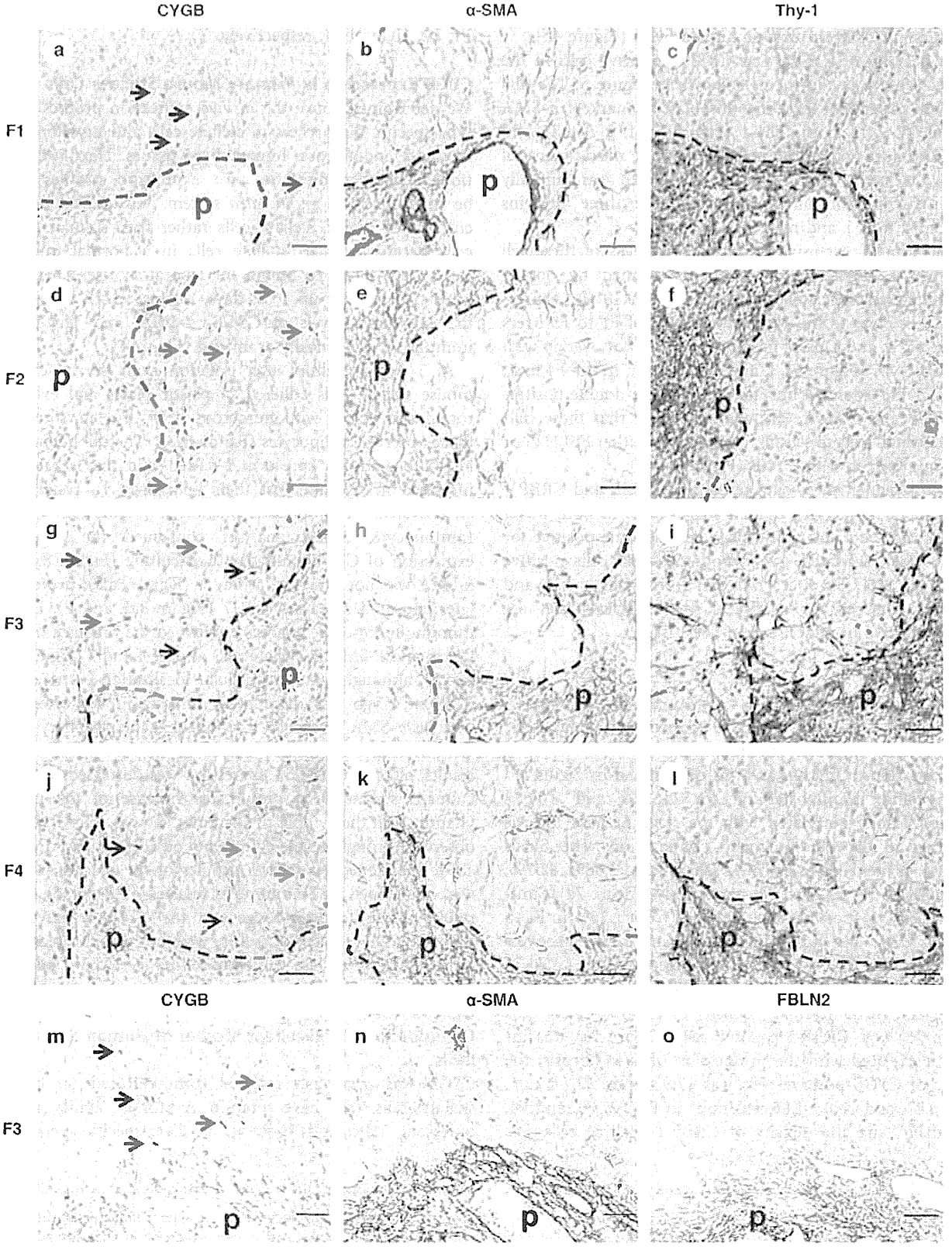
CYGB
α-SMA
Thy-1
F1
F2
F3
F4
a
b
c
d
e
f
g
h
i
j
k
l
p
CYGB
α-SMA
FBLN2
F3
m
n
o
p

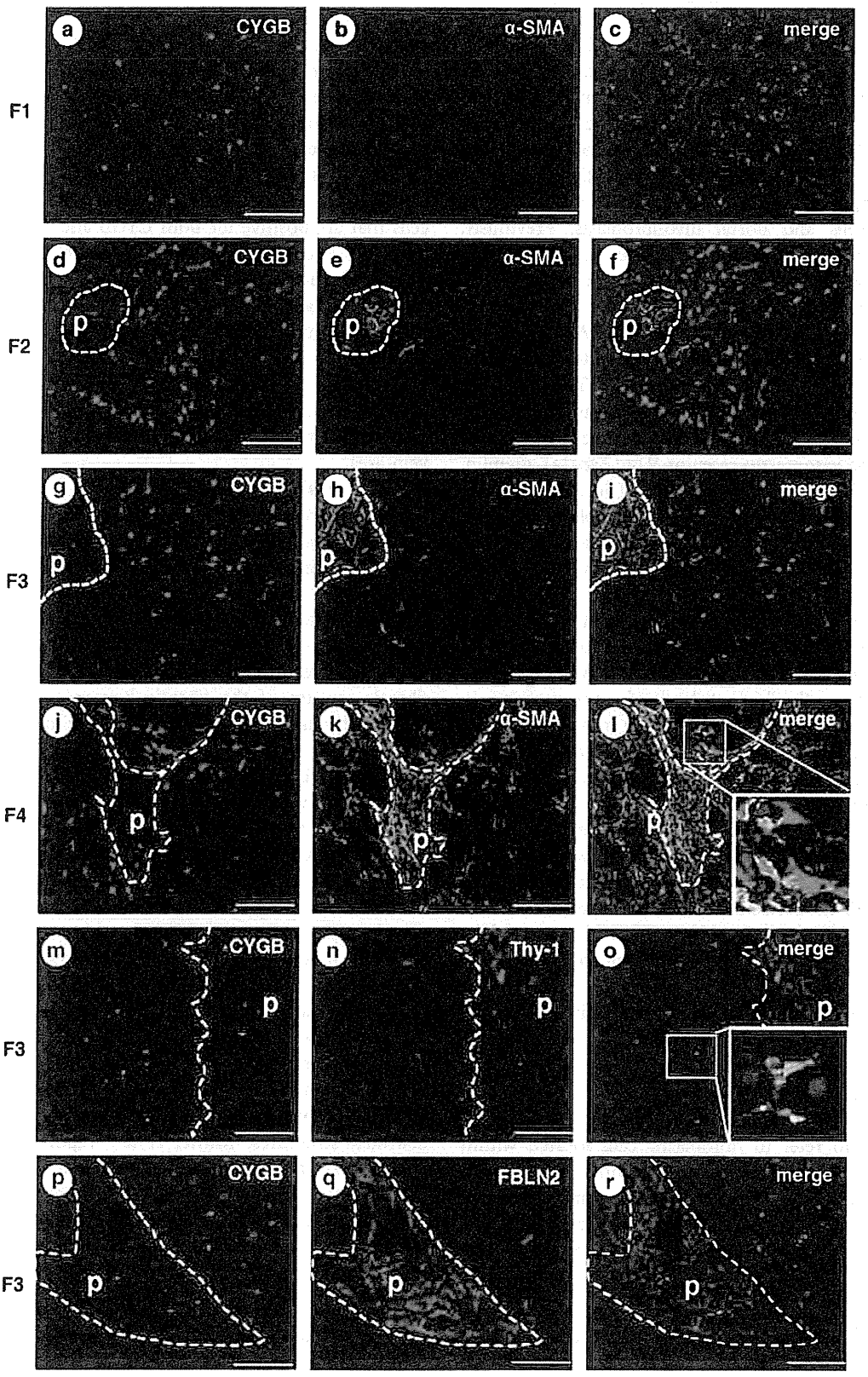
a
CYGB
b
α-SMA
c
merge
F1
d
CYGB
e
α-SMA
f
merge
F2
p
g
CYGB
h
α-SMA
i
merge
F3
p
j
CYGB
k
α-SMA
l
merge
F4
p
m
CYGB
n
Thy-1
o
merge
F3
p
p
CYGB
q
FBLN2
r
merge
F3
p

Histoglobin, CYGB, and stellate cell activation-associated protein were classified as human, mouse, and rat homologs of a hexacoordinate globin that differs from the traditional pentacoordinate globins such as myoglobin and hemoglobin.[1–4] CYGB is induced during the activation of rat hepatic stellate cells, which become myofibroblast-like cells, and its expression is increased in fibrotic livers in rodent models.[1] However, it is unclear whether CYGB is expressed in both stellate cells and portal myofibroblasts. Previously, Ogawa *et al*[21] isolated vitamin A-free cells from the nonparenchymal cell fraction in rat livers using FACS analysis. Ogawa *et al*[21] then demonstrated that vitamin A-positive cells are desmin, CYGB, and α-SMA positive and also highly express oxidized low-density lipoprotein receptor 1, endothelin receptor B, and cardiac troponin T. In contrast, vitamin A-free cells are negative for desmin and CYGB but positive for α-SMA and FBLN2. These cell types express high levels of arginine vasopressin receptor V1a (Avpr1a), gremlin, osteopontin, collagen a3(V), and lumican. Thus, Ogawa *et al*[21] concluded that CYGB could be a promising molecular marker of rat hepatic stellate cells. Furthermore, Bosselut *et al*[29] performed a comparative proteomic study to identify markers and gain insight into the distinct functions of myofibroblasts derived from either hepatic stellate cells or portal mesenchymal cells in rats.[21] The two cell types were subjected to comparative analyses by 2-D MS/MS. CYGB was confirmed to have the highest level of overexpression in activated stellate cells, as confirmed by reverse-transcription quantitative real-time PCR, immunoblot, and immunocytochemical analyses. Thus, CYGB was identified as the best marker for distinguishing stellate cells from portal myofibroblasts. The results also suggested different functions for the two cell populations in the liver wound-healing response, with a prominent role for portal myofibroblasts in scar formation. It should be noted that these previous studies confirmed the expression of CYGB in rodent hepatic stellate cells and *in vivo* models, whereas the present study addressed the actual localization of CYGB in human stellate cells, but not in portal myofibroblasts that are positive for FBLN2 and Thy-1.

Definition of Hepatic Myofibroblasts

The term 'myofibroblast' was first proposed by Gabbiani *et al*[30] in 1972 to refer to fibroblastic cells located within granulation tissue that exhibit substantial cytoplasmic microfilaments composed of actin, myosin, and associated proteins.[29] In particular, the microfilaments of myofibroblasts contain α-SMA that is the actin isoform typical of smooth muscle cells located in the vessel wall[30] and has become the most reliable marker for myofibroblastic cells.[31,32] Myofibroblasts are additionally positive for Thy-1.[12,13]

In the liver, hepatic stellate cells and portal fibroblasts are able to acquire a myofibroblastic phenotype,[8,33] although it has remained difficult to distinguish myofibroblastic (activated) stellate cells from portal myofibroblasts in human liver tissue. In the current study, we showed that cells that are positive for both CYGB and CRBP-1 represent the quiescent phenotype of human stellate cells that are uniquely localized in the perisinusoidal space, and cells that are additionally positive for α-SMA are myofibroblastic (activated) human stellate cells that are predominantly present near the fibrotic septum of advanced fibrotic liver tissues. Furthermore, we observed that cells positive for Thy-1 and FBLN2 in normal liver tissues (ie, portal myofibroblasts) were present but scarce around the portal vein area.

Dudas *et al*[12] first reported that Thy-1 is an *in vivo* and *in vitro* marker of rat hepatic myofibroblasts, and later confirmed that Thy-1 is not present in normal or capillarized sinusoids or in isolated rat stellate cells, and that it is neither inducible in isolated stellate cells nor upregulated in myofibroblasts.[14] In accordance with this report, we detected Thy-1 positivity to a limited extent around the portal vein area in the intact human liver and in the extended fibrotic septum of the fibrotic human liver, where portal myofibroblasts are located. Culture experiments using mouse stellate cells confirmed that these cells express CYGB throughout the culture period until day 7 and α-SMA at days 4 and 7, whereas Thy-1 is not expressed throughout this period. Thus, our data also support the hypothesis that Thy-1 is not a marker of hepatic stellate cells in humans or mice, although it is expressed in myofibroblasts around the portal vein area. The reason for the minimal expression of Thy-1 in portal myofibroblasts is not known, although Thy-1 regulates fibroblast focal adhesions, cytoskeletal organization, and cell migration.[34]

FBLN2 is an extracellular matrix protein of the fibulin family that binds various extracellular ligands and calcium. FBLN2 is present in the basement membrane and stroma of several tissues and may play a role in organ development, particularly during the differentiation of heart, skeletal, and neuronal structures. Knittel *et al*[15] reported that FBLN2-positive MFs are detectable in the portal field, vessel walls, and hepatic parenchyma of the normal liver, and their number is increased in the septal regions during liver fibrogenesis in rat models. These findings are similar to

Figure 6 Double immunofluorescence staining. CYGB (red in panels **a**, **d**, **g**, and **j**; green in panels **m** and **p**), α-SMA (green in panels **b**, **e**, **h**, and **k**), DAPI (blue), Thy-1 (red in panel **n**), and FBLN2 (red in panel **q**) are shown. Merged photographs of CYGB and α-SMA, FBLN2, or Thy-1 are also presented. CYGB was expressed in the parenchyma and inside hepatocytic nodules. Cells constituting the fibrotic septum in advanced fibrosis (F3) were positive for α-SMA but negative for CYGB. CYGB and α-SMA double-positive cells were occasionally present around the fibrotic septum of F4 liver (**i**). CYGB-positive cells did not overlap with cells that were positive for Thy-1 or FBLN2 (**o** and **r**). Bar, 100 μm.

our present observations in diseased human livers. Thus, FBLN2 and Thy-1 are reliable cellular markers of portal myofibroblasts that differ from stellate cells that are positive for CYGB and CRBP-1 in intact and fibrotic human livers. In the portal area, MFs that are negative for CYGB are the main cells that induce fibrotic septum formation. Thus, targeting of these cells in addition to stellate cells has therapeutic potential for controlling fibrotic septum development.

Cellular Markers of Hepatic Stellate Cells

Based on our present results, we emphasize the superiority of CYGB as a marker of human stellate cells in both intact and fibrotic livers. Several markers of stellate cells have been reported in rodents and humans. Stellate cells store vitamin A-containing lipid droplets, suggesting that vitamin A may be a useful marker of stellate cells.[35] However, a specific staining method to identify vitamin A or related compounds,

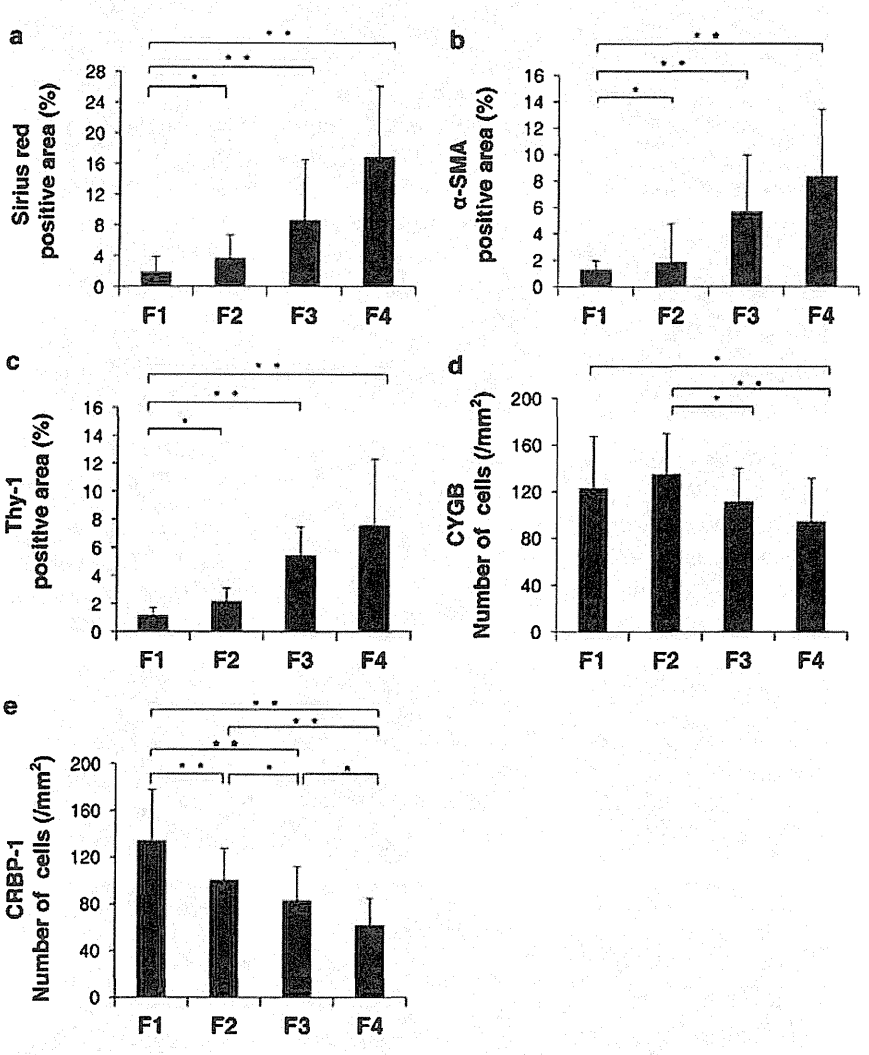

Figure 7 Morphometric analysis. (**a–c**) Correlation between hepatic fibrosis stage (according to the new Inuyama classification) and the ratio of the Sirius red-positive area (**a**), α-SMA-positive area, (**b**) or Thy-1-positive area (**c**). Positive areas for Sirius red, α-SMA, or Thy-1 immunohistochemistry were determined using Lumina Vision 2.4 bio-imaging software (Mitani Corporation, Tokyo, Japan). Note that the Sirius red-positive area, α-SMA-positive area, and Thy-1-positive area increased with the progression of liver fibrosis. (**d**, **e**) CYGB or CRBP-1-positive cells were counted in a 1.4 mm^2 area under a × 100 objective. Note that the CYGB- and CRBP-1-positive cell numbers decreased as liver fibrosis progressed. $^*P<0.05$, $^{**}P<0.01$.

Figure 8 CYGB expression in primary cultured mouse stellate cells. After 1 day of culture following isolation, mouse HSCs adhered to plastic plates and exhibited round cell bodies with numerous lipid droplets similar to those observed in lipocytes. Cell bodies then began to gradually spread and flatten, increasing in size and losing lipid droplets, resulting in the activated myofibroblastic phenotype. (**a**) Immunocytochemical analyses confirmed the expression of CYGB throughout the experimental period (A–C), and α-SMA was detected at days 4 and 7 (D–F). Double immunofluorescence showed that activated mouse stellate cells were positive for both Cygb and α-SMA (G, H, I). Under identical culture conditions, Thy-1 was not observed in mouse stellate cells (M, N, O) that were positive for Cygb (J–L, P–R). Bar, 20 μm. (**b**) Immunoblot analyses confirmed the presence of CYGB at days 1, 4, and 7 and α-SMA at days 4 and 7. Thy-1 was not detected throughout the culture period.

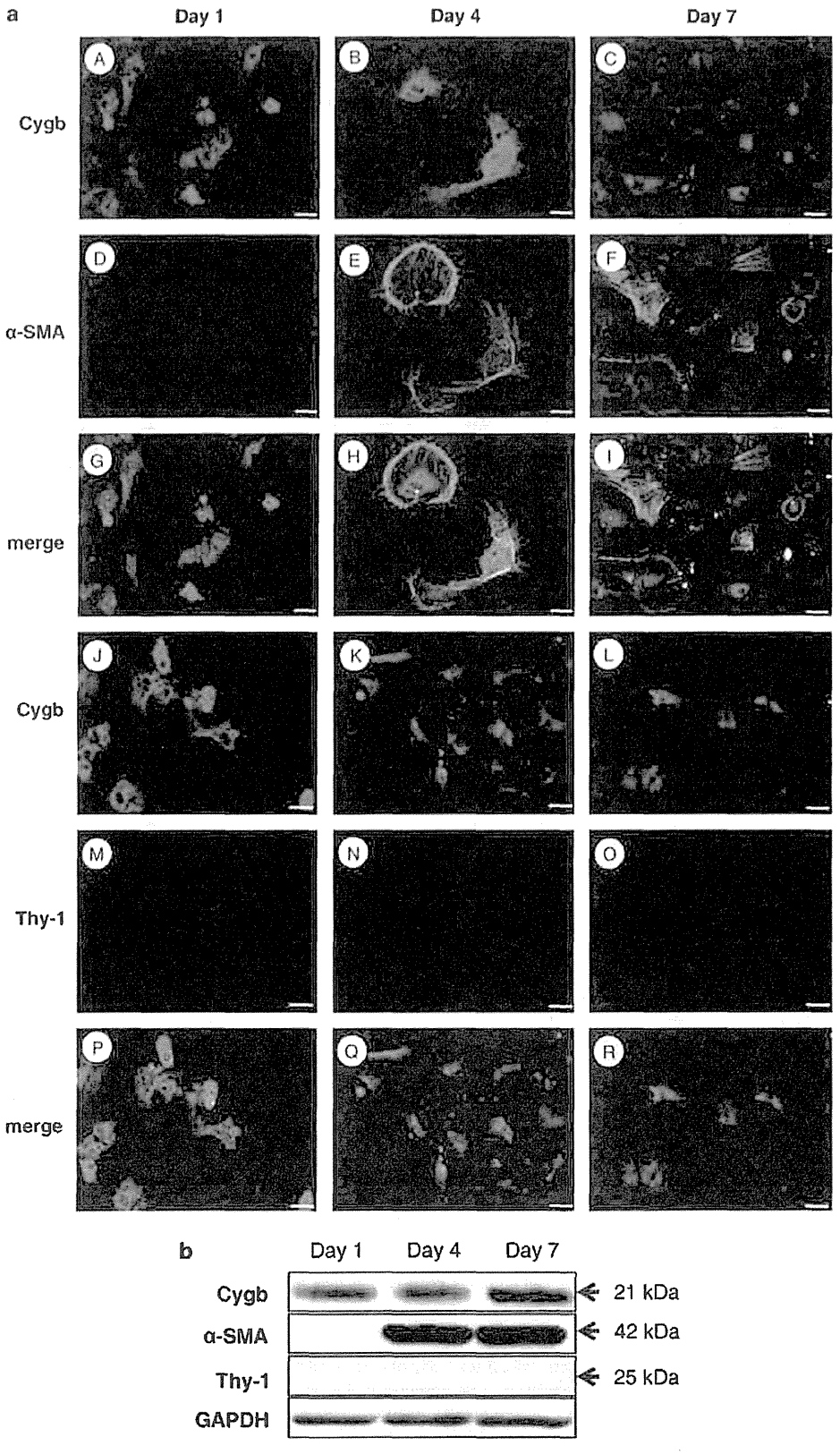
a
Day 1
Day 4
Day 7
Cygb
α-SMA
merge
Cygb
Thy-1
merge
A
B
C
D
E
F
G
H
I
J
K
L
M
N
O
P
Q
R
b
Day 1
Day 4
Day 7
Cygb
α-SMA
Thy-1
GAPDH
21 kDa
42 kDa
25 kDa

such as retinol and retinoic acid, has not been developed, and detection of these compounds via fluorescence microscopy is inconvenient for fixed human liver tissues obtained via clinical procedures. In this context, the use of CRBP-1, a carrier protein of intracellular retinol, is reasonable.[11] CRBP-1 was observed to be downregulated in human livers with advanced fibrosis (Figure 7), presumably because of the loss of vitamin A in stellate cells upon cell activation.

As discussed above, α-SMA is frequently used as a marker of activated and myofibroblastic stellate cells.[29–33] However, this cytoskeletal protein is also expressed in portal myofibroblasts and vascular smooth muscle cells in the arteries, portal vein, and central veins, indicating that α-SMA is not specific for stellate cells. Vinculin, a membrane-cytoskeletal protein in focal adhesion plaques, and synemin, an intermediate filament, show localization patterns similar to that of α-SMA.[36,37]

Desmin, a 52 kD protein that is a subunit of intermediate filaments in skeletal muscle, smooth muscle, and cardiac muscle, was originally identified as a stellate cell marker by Yokoi *et al*[10] in 1984. Desmin is clearly detectable in mouse and rat stellate cells in tissue and in primary culture but not expressed by human stellate cells. Furthermore, desmin expression in rodent hepatic stellate cells has been reported to be both heterogeneous and location dependent.[38] Thus, desmin is no longer considered to be a specific marker of stellate cells. Although neural cell adhesion molecule (also known as CD56) and the intermediate proteins glial fibrillary acidic protein and vimentin have frequently been used as markers of stellate cells, these proteins are also expressed by myofibroblasts.[39,40] In addition, although neurotrophin-3 is specific for stellate cells, it disappears in activated stellate cells in human tissue.[41]

CONCLUSIONS

Taken together, our findings reveal that CYGB is an excellent marker for quiescent and activated stellate cells in both intact and fibrotic human liver. Because the identity of the cell types that participate in collagen production and the fibrotic process in the diseased human liver (caused by hepatitis B or C virus infection, alcohol abuse, obesity, or autoimmune disease) is controversial and because myofibroblasts can be derived from stellate cells, portal myofibroblasts, mesothelial cells,[42] and the epithelial–mesenchymal transition,[43] a molecular marker that is able to uniquely trace stellate cells inhuman liver tissues will be valuable for studying the pathogenesis and fibrotic process of human liver disease.

ACKNOWLEDGMENTS

We thank Professor Kazuo Ikeda and Dr Keiko Iwaisako, Osaka City University Medical School, for their valuable comments on this study. This work was supported by a Grant-in-Aid for Scientific Research from the Japan Society for the Promotion of Science (JSPS) (no. 21390232; 2009–2011; to NK); a grant from the Ministry of Health, Labour, and Welfare of Japan (2008–2010; to NK); and a Thrust Area Research Grant from Osaka City University (2008–2012; to NK).

DISCLOSURE/CONFLICT OF INTEREST

The authors declare no conflict of interest.

1. Kawada N, Kristensen DB, Asahina K, *et al.* Characterization of a stellate cell activation-associated protein (STAP) with peroxidase activity found in rat hepatic stellate cells. J Biol Chem 2001;276:25318–25323.
2. Trent 3rd JT, Hargrove MS. A ubiquitously expressed human hexacoordinate hemoglobin. J Biol Chem 2002;277:19538–19545.
3. Burmester T, Ebner B, Weich B, *et al.* Cytoglobin: a novel globin type ubiquitously expressed in vertebrate tissues. Mol Biol Evol 2002;19:416–421.
4. Pesce A, Bolognesi M, Bocedi A, *et al.* Neuroglobin and cytoglobin. Fresh blood for the vertebrate globin family. EMBO Rep 2002;3:1146–1151.
5. Sawai H, Kawada N, Yoshizato K, *et al.* Characterization of the heme environmental structure of cytoglobin, a fourth globin in humans. Biochemistry 2003;42:5133–5142.
6. Schmidt M, Gerlach F, Avivi A, *et al.* Cytoglobin is a respiratory protein in connective tissue and neurons, which is up-regulated by hypoxia. J Biol Chem 2004;279:8063–8069.
7. Geuens E, Brouns I, Flamez D, *et al.* A globin in the nucleus! J Biol Chem 2003;278:30417–30420.
8. Friedman SL. Hepatic stellate cells: protean, multifunctional, and enigmatic cells of the liver. Physiol Rev. 2008;88:125–172.
9. Scholten D, Osterreicher CH, Scholten A, *et al.* Genetic labeling does not detect epithelial-to-mesenchymal transition of cholangiocytes in liver fibrosis in mice. Gastroenterology 2010;139:987–998.
10. Yokoi Y, Namihisa T, Kuroda H, *et al.* Immunocytochemical detection of desmin in fat-storing cells (Ito cells). Hepatology 1984;4:709–714.
11. Uchio K, Tuchweber B, Manabe N, *et al.* Cellular retinol-binding protein-1 expression and modulation during in vivo and in vitro myofibroblastic differentiation of rat hepatic stellate cells and portal fibroblasts. Lab Invest 2002;82:619–628.
12. Dudas J, Mansuroglu T, Batusic D, *et al.* Thy-1 is an in vivo and in vitro marker of liver myofibroblasts. Cell Tissue Res 2007;329:503–514.
13. Dezso K, Jelnes P, László V, *et al.* Thy-1 is expressed in hepatic myofibroblasts and not oval cells in stem cell-mediated liver regeneration. Am J Pathol 2007;171:1529–1537.
14. Dudas J, Mansuroglu T, Batusic D, *et al.* Thy-1 is expressed in myofibroblasts but not found in hepatic stellate cells following liver injury. Histochem Cell Biol 2009;131:115–127.
15. Knittel T, Kobold D, Saile B, *et al.* Rat liver myofibroblasts and hepatic stellate cells: different cell populations of the fibroblast lineage with fibrogenic potential. Gastroenterology 1999;117:1205–1221.
16. Uyama N, Iimuro Y, Kawada N, *et al.* Fascin, a novel marker of human hepatic stellate cells, may regulate their proliferation, migration, and collagen gene expression through the FAK-PI3K-Akt pathway. Lab Invest 2012;92:57–71.
17. Piscaglia F, Dudás J, Knittel T, *et al.* Expression of ECM proteins fibulin-1 and -2 in acute and chronic liver disease and in cultured rat liver cells. Cell Tissue Res 2009;337:449–462.
18. Janiec DJ, Jacobson ER, Freeth A, *et al.* Histologic variation of grade and stage of non-alcoholic fatty liver disease in liver biopsies. Obes Surg 2005;15:497–501.
19. Ichida F, Tsuji T, Omata M, *et al.* New Inuyama classification; new criteria for histological assessment of chronic hepatitis. Int Hepatol Com 1996;6:112–119.
20. Mori M, Fujii H, Ogawa T, *et al.* Close correlation of liver stiffness with collagen deposition and presence of myofibroblasts in non-alcoholic fatty liver disease. Hepatol Res 2011;41:897–903.
21. Ogawa T, Tateno C, Asahina K, *et al.* Identification of vitamin A-free cells in a stellate cell-enriched fraction of normal rat liver as myofibroblasts. Histochem Cell Biol 2007;127:161–174.
22. Xu L, Hui AY, Albanis E, *et al.* Human hepatic stellate cell lines, LX-1 and LX-2: new tools for analysis of hepatic fibrosis. Gut 2005;54:142–151.
23. Kristensen DB, Kawada N, Imamura K, *et al.* Proteome analysis of rat hepatic stellate cells. Hepatology 2000;32:268–277.
24. Mu YP, Ogawa T, Kawada N. Reversibility of fibrosis, inflammation, and endoplasmic reticulum stress in the liver of rats fed a methionine-choline-deficient diet. Lab Invest 2010;90:245–256.